Fibers and Polymers 2020, Vol.21, No.12, 2753-2768
DOI 10.1007/s12221-020-1000-8

ISSN 1229-9197 (print version)
ISSN 1875-0052 (electronic version)

Study on Morphology, Thermal and Rheological Properties of Polypropylene/Poly(trimethylene terephthalate) Polyblend Fibers

Mohammad Reza Habibolah Zargar[1]*, Atefeh Ghaffarian[2], Amin Ebrahimzade[1], and Ahmad Mousavi Shoushtari[1]

[1]*Department of Textile Engineering, Amirkabir University of Technology (Tehran Polytechnic), Tehran 15875-4413, Iran*
[2]*Department of Art, Science and Culture University, Tehran 1461968151, Iran*
(Received November 4, 2018; Revised March 2, 2020; Accepted March 16, 2020)

Abstract: In the present work, a systematic study of the variables affecting the production of polypropylene (PP)/ poly(trimethylene terephthalate) (PTT) blend fibers such as the PTT and PP-g-MA compatibleizer ratios and take-up speed in the melt-spinning process was done. Modeling of the melt-spinning process was carried out by using a statistical approach based on response surface methodology (RSM) to achieve a mathematical model. The formation of the fibrillar structures through different steps of fiber formation was confirmed by scanning electron microscopy (SEM). The lowest mean diameter of nano-fibrils was achieved to be 63 nm, for the hot-drawn fibers consisting of 10 wt.% of PTT. The synergetic effect of the presence of PTT dispersed phase on the mechanical properties of PP fibers as a matrix was verified by observing a positive deviation from the blends linear law for the samples with 10 wt.% of PTT. The rheological evaluations suggested the formation of a fibril structure in the blends. The X-ray diffraction spectroscopy and DSC results showed that the presence of PTT significantly influenced the crystallinity of PP. Moreover, results indicated that the average crystal size of the PP matrix phase was affected by the presence of the PTT dispersed phase, which also confirmed its nucleating effect in the blend.

Keywords: Polypropylene, Poly(trimethylene terephthalate), Blend, Melt-spinning

Introduction

PP fibers have become one of the fastest and largest growing synthetic fibers owing to such advantages as low price, great mechanical property and resistance to many chemical material [1,2]. Nevertheless, PP fibers have some limitations, such as lack of a resiliency and poor dye ability. Although there are many researches about more applications of modified PP by plasma modification, blending with other polymers and impregnation with nano-material. Blending process with suitable polymer seems cheaper and more environmental favorable, and so generally embraced and widely applied [3].

Since PP is immiscible with most long-chain thermoplastic polymers, the compatibilizers must be added during the blending process to increase the dispersion of the incompatible blend component and to make adhesive interfacial between the dispersed micro-phases and the polymer matrix [4]. Rosch *et al.* [5] showed that styrene-ethylene-butylene-styrene which is grafted with maleic anhydride (SEBS-g-MA) gives much finer dispersions of the micro phases in PP matrix as a compatibilizer. However, PP-g-MA produces spherical dispersed micro phases with separate phase borders. The increase of PP-g-MA contents the average diameter of the spheres decreases while the type of morphology remains stable. In conflict, the increase of SEBS-g-MA leads to constitution of irregular shaped honey-comb type particles micro phases and the particles are agglomerated to appearance clusters of such core/shell. Tao *et al.* [6] studied the crystallization behavior in compatibilized PP (recycled)/ polyethylene terephthalate (PET) blends and evaluated that the crystallization rate follows this order: PP grafted acrylic acid (PP-g-AA) > PP grafted glycidyl methacrylate (PP-g-GMA) > PP grafted maleic anhydride (PP-g-MA). Dobrovszky *et al.* [7] resulted that suitable selection of an efficient compatibilizer is important to avoid the reduction of mechanical properties of blends. The accurate amount of compatibilizer should be determined to obtain the best blend fibers. The various literatures indicated that the role of PP-g-MA in the improvement of the compatibility of the blend polymers as major polymer component has been evaluated in range of 1 to 5 % limited extend. Further addition *i.e.* 5 % PP-g-MA compatibleizer led to reduce mechanical properties [8-10].

Poly(trimethylene terephthalate) (PTT) has recently encouraged many investigators to these properties either in pristine and blend state. This polymer has favorable resiliency behavior, and easy dyeability at low temperatures (lower 100 ^{o}C). The special zigzag molecular chain conformation of PTT is the main reason for the particular interest in this polymer during recent years. It is clear that the development of the fibril structures of PTT disperse phase in PP matrix at blending process could affect noticeably the mechanical properties and resilience behavior of blend fibers [11]. However, the price of PTT is higher than that of conventional textile polymers and the density of this polymer is high and it's elastic modulus is a bit lower than other textile polymers [12-15].

The main aim of this research is to deal with one of major drawbacks of PP fibers by blending process. The

*Corresponding author: mrh.zargar@yahoo.com

development of the fibril structures of PTT as a dispersing segment into the PP polymer matrix can affect noticeably mechanical properties, rheological and thermal behavior of the fibers. Lin *et al.* [16] showed that PTT could inhibit the formation of β-crystal in phase PP. From the results, it could be concluded that the β-crystal containing PP phase in the PP/PTT blends decreased when the amount of PTT increased. But Liu *et al.* [17] reported that the addition of Acrylonitrile-butadiene-styrene (ABS) as compatiblizer could improve the formation of the PP β-crystal. Ujhelyiova *et al.* [18] investigated that for production of dyeable PP fibers, a small amount of less crystalline polymers such as PTT can be added into PP through melt spinning process. Also, they reported that PP-g-MA compatibleizer did not result any significant toughness improvement of blend, but the tensile strength was raised up considerably. Lin *et al.* [19] demonstrated that PTT/PP blends with higher amount of PP caused to higher degradation temperature based on TGA analyses.

The main goal of this study is industrial scale investigation of spin-ability and fabrication of PP/PTT blend fibers by PP-g-MA compatibleizer. We suggest the optimized PP/PP-g-MA/PTT content prepared fibers produced in this study will be a promising candidate for a wide range of engineering applications (*e.g.*, apparel, garments and carpets) in the near future.

Experimental

Materials

All of the materials in this research were of commercial grade. Isotactic polypropylene (PP) (552R, Arak Petrochemical, Co., Iran), with melt flow index (MFI) of 28 g/10 min at 230 °C and 2.16 kg was used as the matrix phase., South Korea with 1.5 % degree of grafting and MFI 50 g/10 min at 230 °C and 2.16 kg, and made use of as the compatibilizing agent. PTT pellets (Corterra 9200, Shell Chemical Co., USA), with an intrinsic viscosity (I.V.) and weight averaged molecular weights of about 0.92 dl/g, and 78,100 Da, respectively, were utilized as the dispersed phase in the blends. Analytical grade decahydronaphthalene (Decalin, Merck Co., Germany) was used as a matrix phase solvent of the blend fiber samples for study of the PTT morphology (as the dispersed phase) by scanning electron microscopy (SEM).

Blend Preparation

The PP-g-MA and PTT pellets were dried with N_2 purging in a laboratory dryer for 8 h at 140 °C prior to melt-mixing so as to avoid moisture-induced degradation and hydrolysis. The PP/PP-g-MA/PTT masterbatch blend samples were prepared in a co-rotating twin-screw extruder (PL 2000; Brabender GmbH & Co., Germany) at a screw speed of 100 rpm and a feed rate of 4 kg/h under nitrogen atmosphere. The temperatures from the hopper to the die were 210 °C, 220 °C, 240 °C, 250 °C, and 250 °C, respectively. The resulting products were cut into pellets.

Melt-spinning Process for Producing Pristine and Blended Fiber Samples

Melt-spinning was applied in a semi-industrial machine (Automatic Co., Germany) to produce pristine and blend fiber samples. There was a single-screw extruder (L/D=25, D=35 mm with L and D being the length and diameter of the screw) equipped with a static mixer and a die section that was coupled to a spinneret unit having 36 circular holes (each of 0.25 mm diameter) under nitrogen atmosphere. The applied barrel temperature profile between feeding zone and spinneret orifice zone was 240, 245, 250, 255 and 260 °C, respectively. The extruded fibers were then air-cooled simultaneously. Low Oriented Yarn (LOY) or as as-spun yarn samples fibers have been prepared at the take-up speed from 1000 to 1600 m/min with a good constant spin-ability regardless of composition. It should be noted that though the PP and PTT are immiscible and their combination can be achieved by adding PP-g-MA as a compatibleizer in high take-up speed through melt spinning processes. Fully Drawn Yarns (FDY) have been also manufactured by hot drawing process.

After the melt spinning process of fiber, the LOY fibers applied on hot drawing process at a speed of 400 m/min by an industrial drawing machine (Zinser Co., Germany) equipped with hot godet rolls (60 °C) and a hot plate (140 °C). Draw ratios (D.R.) were set on (~2.7) regarding to LOY stress-strain curves of the samples (40±5 % residual elongation at break) based on our prior research [11,12].

In pre-experimental procedure, no blend had higher than 15 wt.% PTT dispersed phase content since the blend products were prepared at above the take-up speed around 1300 m/min so that these can't have a good constant spinnability. The blending ratios of PP/PP-g-MA/PTT for the various LOY fiber samples were 91/4/5, 86/4/10, 81/4/15, 76/4/20 by weight percent at 1000 m/min take up speeds in the melt-spinning process. We note that in this procedure it is not possible to produce blend fibers with take-up speeds of 1600 m/min and higher for PTT dispersed phase (PDP) contents of 15 wt.% and higher, showing that these samples did not have good spinnability.

Design of Experiments

Modeling of the melt-spinning process were carried out by using a statistical approach based on the response surface methodology (RSM) to achieve a mathematical model, by which predicting the mechanical properties of PP/PP-g-MA/PTT blend fibers could be possible. RSM is an experimental statistical modeling method employed for multiple regression analysis using quantitative data obtained from suitable designed experiments to appraise the relationship between a

Table 1. Independent variables used in experimental design and their levels in actual and coded values

Parameters	Parameters description	Low level actual	High level actual	Low level coded	High level coded
X_1	Concentration of PTT (%)	5	15	-1	+1
X_2	Concentration of PP-g-MAH (%)	3	5	-1	+1
X_3	Take-up speed (m/min)	1000	1600	-1	+1

set of controllable experimental factors and solve multivariate equation simultaneously [20]. Therefore, in the present work, a systematic study of the variables affecting the production of PP/PP-g-MA/PTT blend fibers such as the PTT and PP-g-MA ratios and take-up speed in the melt-spinning process were done. A Box-Behnken Design (BBD) including five replicates at central point, was examined in order to study the effects of three independent parameters are called: concentration of PTT and PP-g-MA (X1, X2, mass %) and take-up speed (X3, m/min) respectively. Because of keeping constant spin ability and making acceptable mechanical properties under industrial scale. The boundary condition of each parameter was chosen based on the results of the pre-experiments as presented in Table 1. In the present research, Design Expert (trial version 8.0) software was applied to assess the values of applied parameters in each test and analysis of the obtained data.

Evaluation of Rheological Behavior

All samples were dried in a laboratory dryer with N2 purging for 8 h at 140 °C to prevent moisture induced degradation and hydrolysis. The rheological behaviors of the specimens; *e.g.* the complex viscosity and storage modulus were measured using a rheometric mechanical spectrometer (RMS, Paar Physica UDS 200, Austria) equipped with a parallel plate (diameter of 25 mm and a constant 1mm gap in a nitrogen atmosphere chamber). The viscoelastic behaviors of the melt samples were evaluated at frequency range of 0.1 to 100 s^{-1} using strain amplitude of 1 %, proven to be in linear viscosity range by means of strain sweep measurements at temperatures 240 °C under nitrogen atmosphere.

Differential Scanning Calorimetry (DSC)

The melting behaviors of the fiber samples were carried out by a DSC 2010 machine (TA Instruments Co., USA). Indium was employed for the temperature and heat flow calibration some mass of samples around 4 mg were weighed from the test substance. The measurements were taken over a temperature range of 30 to 250 °C, at the heating and cooling rates of 10 °C/min, under nitrogen flow using standard aluminum pans. The DSC tests helped to estimate the melting and crystallization temperatures (T_m, T_c) during the first heating and cooling processes as the temperatures of the peaks of the endo- and exo-thermic curves, respectively. The heat of crystallization, ΔH_c and the heat of fusion, ΔH_m were assessed by integrating the areas ($J \cdot g^{-1}$) under the peaks. The degree of crystallinity (X_C, percentage) was characterized using the Sichina, formula explained in equation (1) [21,22].

$$X_C = \frac{\Delta H_m}{\omega_r \times \Delta H_m^{o}} \times 100 \quad (1)$$

where ω_r mentions the weight fraction in the blends, ΔH_m^{o} describes the heat of fusion for a 100 % crystalline polymer ($J\ g^{-1}$) and is predicted to be 207 $J\ g^{-1}$ for pristine PP and 145.5 $J\ g^{-1}$ for pristine PTT [21].

Morphological Behavior

The morphology of PTT deformed particles as dispersed phase was examined using scanning electron microscopy (SEM, Phillips XL30 model, Netherlands) with 15 kV accelerating voltage. The samples were sputter-coated with platinum before SEM scanning. Final images are recorded randomly magnification as indicated in the SEM micrographs. For this purpose, the samples were taken from following conditions:

i. The PP/PP-g-MA/PTT blend samples which were prepared by melt-compounding process using a twin-screw extruder and then the blend samples were fractured at liquid nitrogen (cryo-fractured) and gold sputtered prior to observation [21].

ii. The PP/PP-g-MA/PTT blend fiber samples which were prepared by melt-spinning process and then these fibers were put in a solution of Decalin at 110 °C for 10 min and then the dissolved PP were extracted by so-called "etching process" [23]. The various residual PTT samples prepared for SEM photographs were taken from following conditions:

(a) The samples directly extruded out from the spinneret orifice (gravity spun blend fibers) where is located between spinneret and winder. It is not allowed to be drawn.

(b) The samples taken from melt-drawn process *i.e.*, LOY fibers.

(c) The samples taken from post hot-drawn process *i.e.*, FDY fibers.

Wide-angle X-ray Diffraction (WAXS)

The crystal structures of the samples were studied with a wide-angle X-ray scattering diffract meter (Equinox 3000, Inel Co., France) by using Cu as anode material with radiation (λ=1.54505 angstrom) in the angle range of 2θ=5-50 ° at a voltage of 40 kV and current of 30 mA to determine the crystal size and D-spacing of the crystalline reflection.

The thickness of the crystallite was determined perpendicular to the reflecting plane using the Scherrer formula [24] described in equation (2):

$$\mathrm{ACS} = \frac{K\lambda}{\beta\cos\theta} \tag{2}$$

where ACS is (apparent crystallite size), K is the Scherrer constant, which was taken to be 0.9, λ is the wavelength, β represents the peak width at half-height of the crystalline reflections (in radians) at 2θ≈14.5 Å and θ is the peak angular position [24].

The degree of crystallinity (Wc, x) based on X-ray diffraction data, was calculated by using the Hermans and Weidingeer formula [24] described in equation (3):

$$W_{C,X} = \frac{I_C}{I_C + K \times I_A} \tag{3}$$

where I_C, I_A and K stand for the integral of scattering intensity of the crystalline, amorphous peak and calibration constant (1.235) [24], respectively.

Mechanical Properties Measurements

The tensile measurements of the pristine and blend fiber samples were studied using a universal tensile testing machine (EMT-3050, Elima, Co., Iran) after conditioning them for 24 h at 25 °C and 65 % relative humidity. The tensile testes were examined on the fiber samples with constant rate of extension (C.R.E). The strain rate of 50 cm/min and initial length of 10 cm and 10 cm for FDY and LOY fibers respectively, were selected for all samples according to the ASTM D 1907 standard method. In the studies of mechanical properties, the main focus was on the average tenacity (cN/tex), elongation (%), modulus (cN/tex), and work of rapture or the area under the stress-strain curve (cN/tex). The initial modulus was calculated from the stress at 0.5 to 1 % deformation on the stress-strain curve. Statistical evaluations of the mechanical parameters were obtained through averaging the measured results of the tests (tenacity and elongation) for each sample. For this purpose, at least 10 measurements were carried out for each sample. The statistical result of the average mechanical parameters *i.e.*, standard deviation and coefficient of variation were calculated by tensile tester software and were finally evaluated with each other by IBM SPSS statistic 22.

Results and Discussion

Rheological Behavior of Evaluation

The most important factor in quantifying the rheological behavior of the molten polymer is shear viscosity, which could reflect the interface interaction variations. The rheological properties of the polymer blends with multiple phases could be significantly affected by their interfacial properties. Therefore, it can be said that a finer dispersed phase through the matrix (by compatibilizer) could cause more stabilized structure and higher viscosity. Also, the rheological properties could reflect some information about blends compatibility and compatibilization effect which could reflect the relationship between rheology, morphology and mechanical properties of the blends [25].

The rheological properties obtained from the RMS test for the pristine polymers and the twin-screwed of their blends were shown in Figures 1(a)-(c) at 240 °C. Among the studied range of the low shear rate (frequency range of 0.1-200 s^{-1}), the melt flow of pristine PTT (granule and fiber samples) illustrated a viscosity upturn and near Newtonian flow behavior compared to that of PP (granule and fiber samples). In the beginning, the melt flow of PTT was decreased very slightly with increasing the shear rate, to declare a slight shear thinning behavior. While at a high shear rate, the contrary trend was observed. Although the viscosity of the pristine PTT sample is approximately three times higher than pristine PP, its deviation from the Newtonian flow behavior cannot be neglected entirely. A similar result was previously noticed by Xue *et al.* [4,25].

A higher deviation was found for pristine PP and PP/PP-g-MA/PTT blend fiber. Also, the fluid behavior of the melt blend samples showed great variation of pristine PTT but it was similar to pristine PP matrix. However, the molten pristine PP and PP/PP-g-MA/PTT blends displayed typical pseudo-plastic flow behavior (Viscosity decreases with shear stress), the PP samples (chips and LOY) exhibit more significant shear thinning behavior at low shear rates. The move-ability of the PP chains in blend samples are limited owing to the existence of PTT phase relative to molten PP, especially upper than 10 wt.% PTT. It would be more powerful than the friction force through the interface of molten and dispersed rigid PTT phases. The same results have been reported by other scientists attributed this behavior to the rigid nature of dispersed phase particles structure (*e.g.* PTT and poly (butylene terephthalate) or PBT) and relative soft nature of PP [25-27].

By assessment of the mentioned results, one may note that the melt viscoelastic behavior of the pristine and blend samples is extremely influenced by processing steps (*i.e.* twin-extrusion and melt-spinning steps). Raising shear rate and take-up speed in the melt-spinning process and the next stages of the process in production process play vital roles in fibril structure formation concurrent with fragments of the polymer chains. Therefore, the observed reduction in the shear viscosity of the pristine PP and pristine PTT spun yarns relative to their granule could be ascribed to the fragments of the polymer chains. Whereas, the shear viscosity of PP/PP-g-MA/PTT blend fiber samples (*i.e.* LOY and FDY blend fibers) were higher than twin-extrude components due to the formation of complete fibril structure which results in enhancement of surface contact of two polymeric phases [23]. Hot drawing process can be seen that has

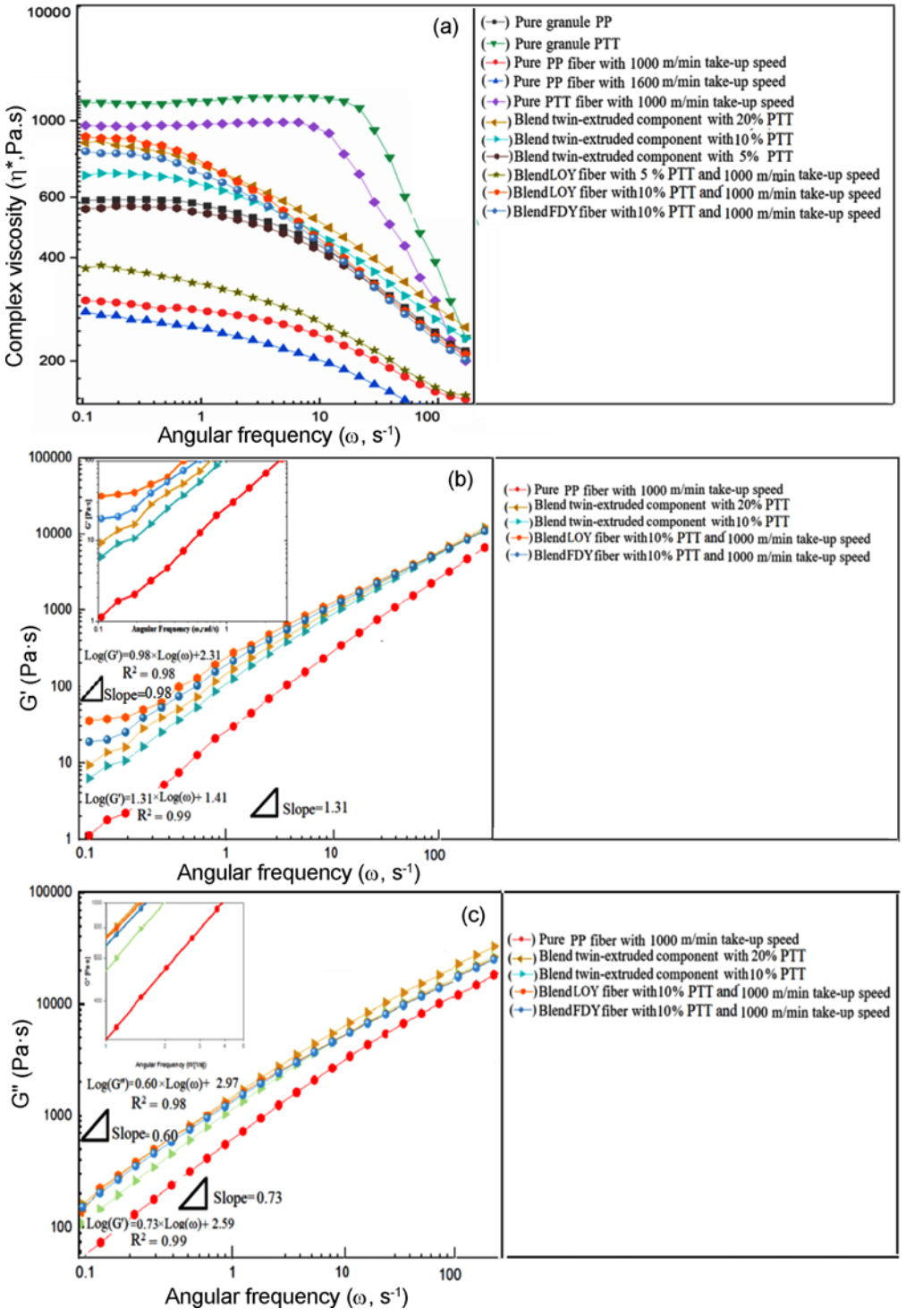

Figure 1. Variation of (a) complex viscosity (b) storage modulus and (c) loss modulus of the samples with frequency at 240 °C.

negligible effect on the viscoelastic behavior of the blend sample. However, the complex viscosity behavior of blended FDY could be reduced as the orientation of microfibers in the direction of draw axis plus entanglements are reduced at higher drawing ratio. Safai *et al.* [28] have worked on the rheological of micro fibril PP/PolyAmid-6 (PA6) composites and they have essentially observed the same outcome.

There is a positive linear relationship between the logarithms of storage modulus (G′) and loss modulus (G″) with the frequency of pristine and blend samples in Figures

1(a)-(c). The rheological behavior of pristine molten PP was observed with liquid-like properties. The slope of the storage modulus (*i.e.* 1.31) and loss modulus (*i.e.* 0.73) of pristine PP fibers are higher than their blends (*i.e.* 0.98 and 0.6 respectively). Moreover, their pristine intercept (*i.e.* 1.41 for G′ and 2.59 for G″ respectively) are smaller than blends (*i.e.* 2.31 for *G′* and 2.97 for G″). The same curves *of* G′ and G″ in melt-blended samples is more than those of the pristine PP. But, the all of blend fiber samples in G′ curves have commonly a plateau at low frequency as shown in Figures 1 (b, c, inset picture). Rizvi *et al.* [29] attributed this slight shift in G′ at low frequencies to the presence of rigid heterogeneities domains *e.g*. PTT that influences the stress relaxation behavior of the matrix. This effect in G′ is more prominent than G″. Exhibit plateau form at low frequencies indicate a transition from liquid-like to solid or gel-like visco-elastic behavior that tends to limit the motion of the matrix polymer chains and prevents them from complete relaxation. It has been allowed to formation of a network of PTT fibrils in the PP matrix.

Morphological Study

Figures 2(a)-(c) show the SEM micrographs and diameter distribution of cryogenically fractured surface of the twin-extruded components for PP/PP-g-MA/PTT (86/4/10: wt.%) and (76/4/20: wt.%). As can be seen, there was a direct relation between the PTT particles size (droplets diameter) and the contents of PTT in the twin-extruded blend samples. When the PTT content was increased to more than 10 wt.% (particularly 20 wt.%), the mean diameter of the PTT particles increased from 2.3 μm to 2.7 μm with more coefficient of variation because of the coalescence of droplets. In addition, there are more small bumps on the fractured interfaces in 10 wt. % PTT blend sample (as shown in Figure 2, a by arrows and inset cay). According to Xue *et al.* [25], these are an evidence of an extended connection between the PP and PTT phases. Whereas, the least adhesion of interfacial interactions is observed in PTT with more than 20 wt.%. These small bumps are attributed to the results of the reactive compatibilization, *i.e.* the reaction between the PTT's hydroxyl groups and the maleic anhydride functional groups of PP formed polymer connections at the interfaces [25]. These SEM morphological consequences revealed that PP-g-MA compatibleizer could develop the interfacial adhesion of PP/PP-g-MA/PTT during melt-blending and as a result it would theoretically enhance its mechanical properties due to adhesion improvement of interfacial interactions. However, by increasing the compatibilizer content the tensile strength is decreased which can be related to its low molecular weight [28].

Likewise, the undrawn PP/PP-g-MA/PTT blend fiber extracted from the spinneret orifice; then these were put in a

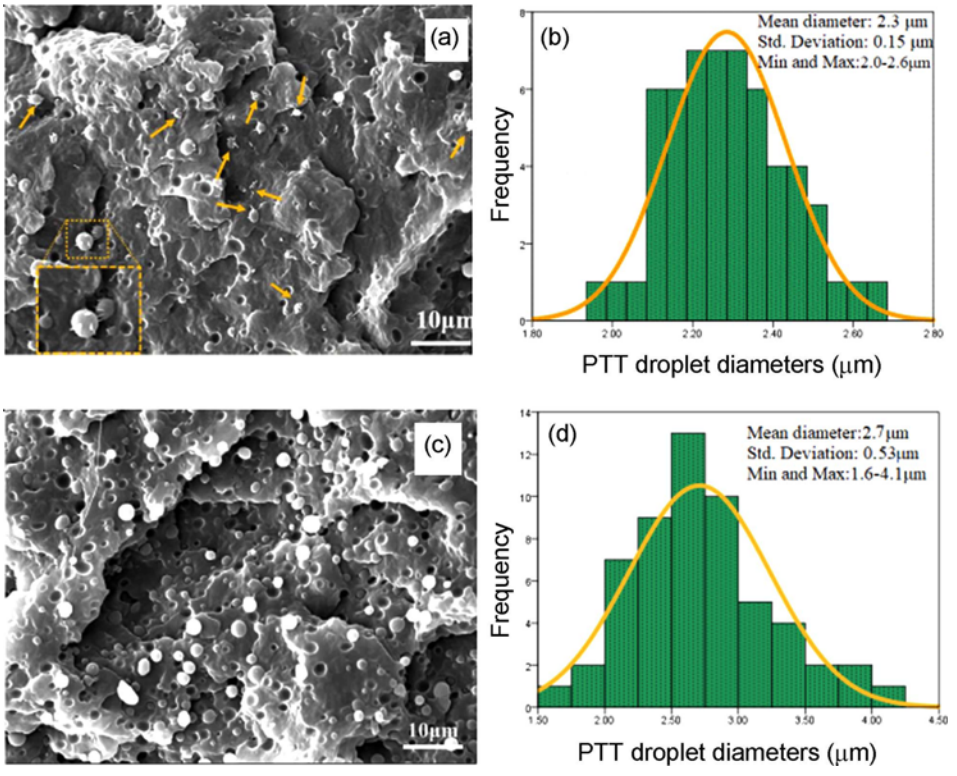

Figure 2. SEM micrographs of the PTT dispersed in PP/PP-g-MAH/PTT blends (a) with 10 (c) 20 % PTT and (b, d) their diameter distribution respectively.

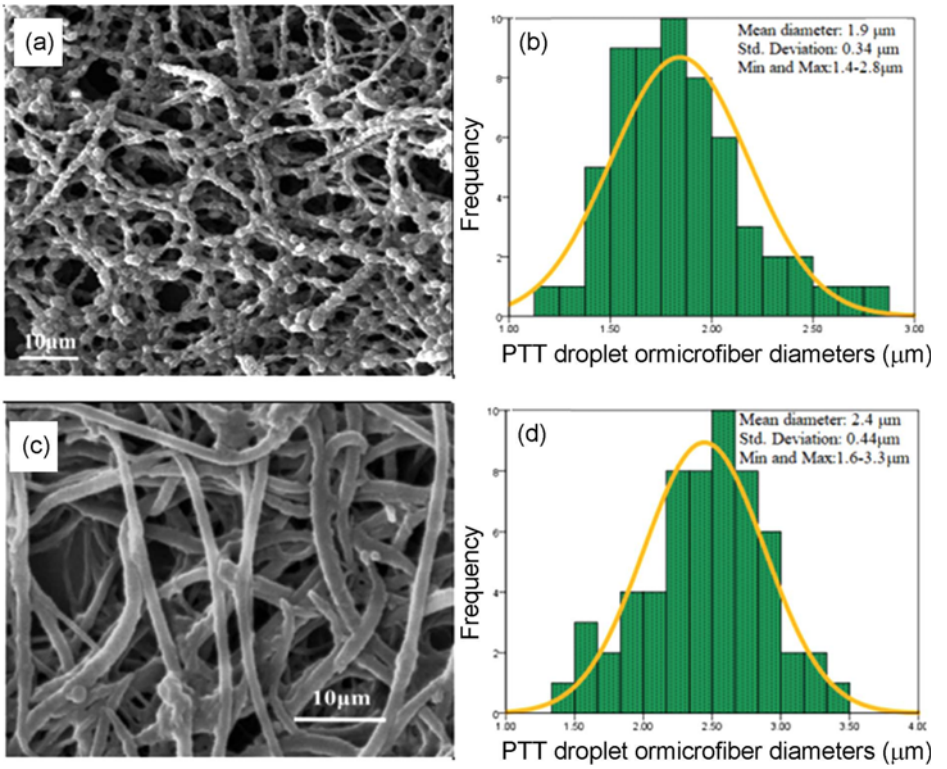

Figure 3. SEM micrographs of the PTT dispersed in the blend fibers (exited from spinneret orifice) after etching process, (a) with 10 (c) 20 % PTT and (b, d) their diameter distribution respectively.

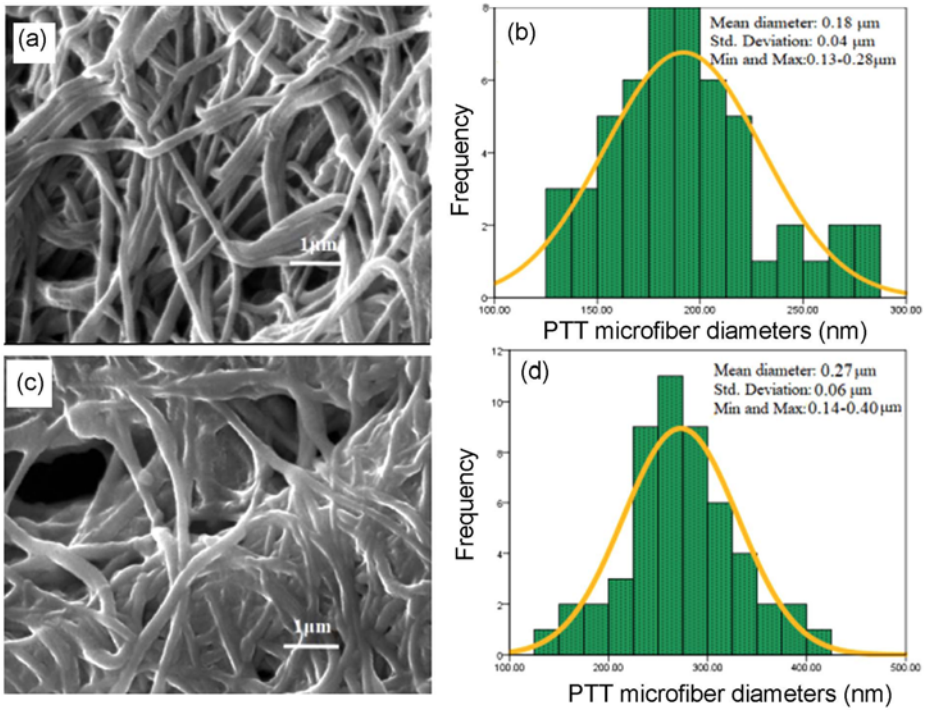

Figure 4. SEM micrographs of the PTT dispersed phase from the as-spun polyblend fibers and 1000 m/min take-up speed) after etching process (a) with 10 (c) 20 % PTT and (b, d) their diameter distribution respectively.

solution of 99 % Decalin at 110 °C for 4 min (etching with decahydronaphtalene). SEM micrographs and diameter distribution of the fibers are shown in Figures 3(a)-(c). As is apparent, the fibril shape was not created for the 10 wt.% of the PTT (*i.e*. beadlike in Figure 3(a)). It seems that the low contents of PTT could prevent in coalescence droplets by the shear flow field in the spinneret orifice. When the PTT content was increased to more than 10 wt.% (particularly 20 wt.%), the form of beadlike was converted to homogeneous fibril without any spherical aberration owning to the coalescence of droplets as shown in Figure 3(c). The same results have been reported previously by Tavanaie *et al.* [23].

In addition, the results of morphological evaluations of the PDP from as spun (LOY fiber), with 1000 m/min take-up speed in the melt spinning process and diameter distributions of nano-fibrils after etching are demonstrated in Figures 4(a)-(d). Due to the coalescence of the PTT particles, with doubling the PTT content to 20 wt.%, the mean diameter of the PTT fibrils improved. This parameter could be affected mechanical properties of the blend fiber [11,12,23,30]. The broad distribution of blend fibers PTT content of 20 wt.% can be related to the non-homogeneity in the PTT droplets. The same results have been reported previously by Tavanaie *et al.* [23] and Afshar *et al.* [31].

Likewise, the results of the morphological studies of the PDP from the DHN etched blend LOY fibers with 10 wt.% PTT amounts, at 1000 and 1600 m/min take-up speed after etching are demonstrated in Figures 4(a) and (b). Figures 5(a) and (b), respectively. The PDP particles were observed as complete fibrils in all of the LOY blend fiber samples. When the take up speed in melt spinning process was increased to more than 1000 m/min (*i.e*. 1600 m/min), the mean diameter of the PTT particles decreased from 0.18 μm to 0.16 μm. It can be attributed to the great, homogenous, elongational stress of the spinning zone between the orifice of spinneret and the take up winding roll in the melt-spinning process [12,29].

In addition, the results of morphological evaluations of the PDP from the DHN etched LOY and FDY fiber with 1600 m/min take-up speed are shown in Figures 5(a)-(d), respectively. The PDP particles were observed as complete fibrils in all of the LOY and FDY blend fiber samples with 1600 m/min take-up speed in the melt spinning process. In the same manner, a considerable decrease in the PTT diameters with the hot drawing (0.16 μm compare to 0.064 μm) as shown in Figures 4(c)-(d). It can be ascribed to the homogeneous elongational stress of the spinning zone between the hot rolls during the heat treatment drawing process.

Thermal Properties Evaluation

The detail of DSC curves of pristine PTT, pristine PP and PP/PP-g-MA/PTT blend were depicted in Figure 6(a). The corresponding crystallization temperature (T_c), melting

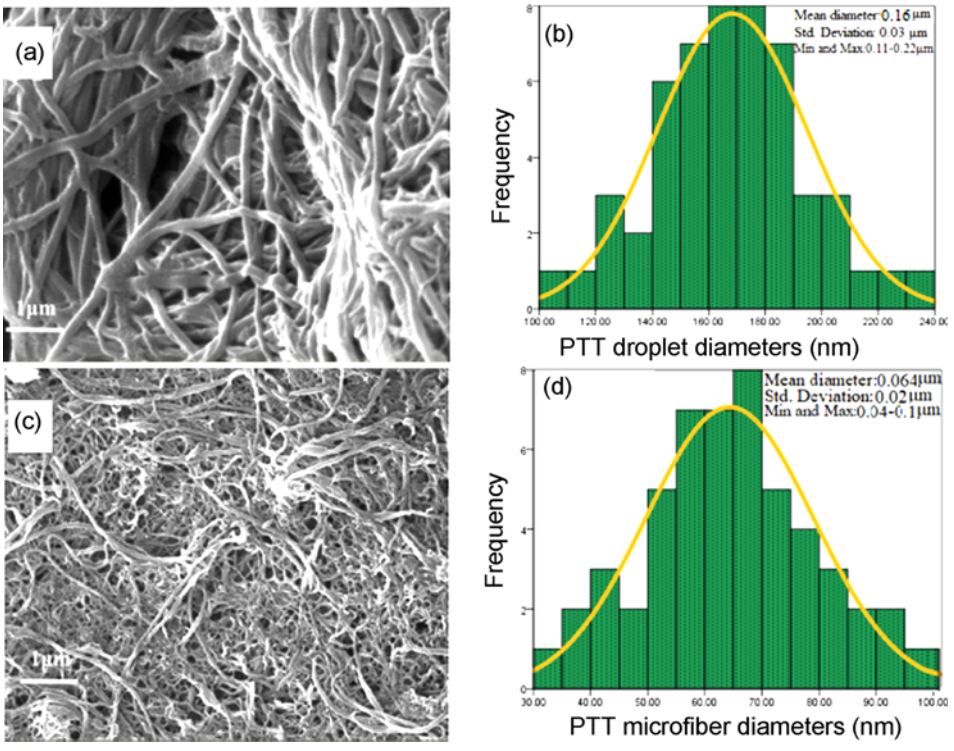

Figure 5. SEM micrographs of the PTT dispersed phase from the polyblend fibers with 10 wt. % PTT and 1600 m/min take-up speed after etching process (a) as spun (LOY) (c) FDY and (b, d) their diameter distribution respectively.

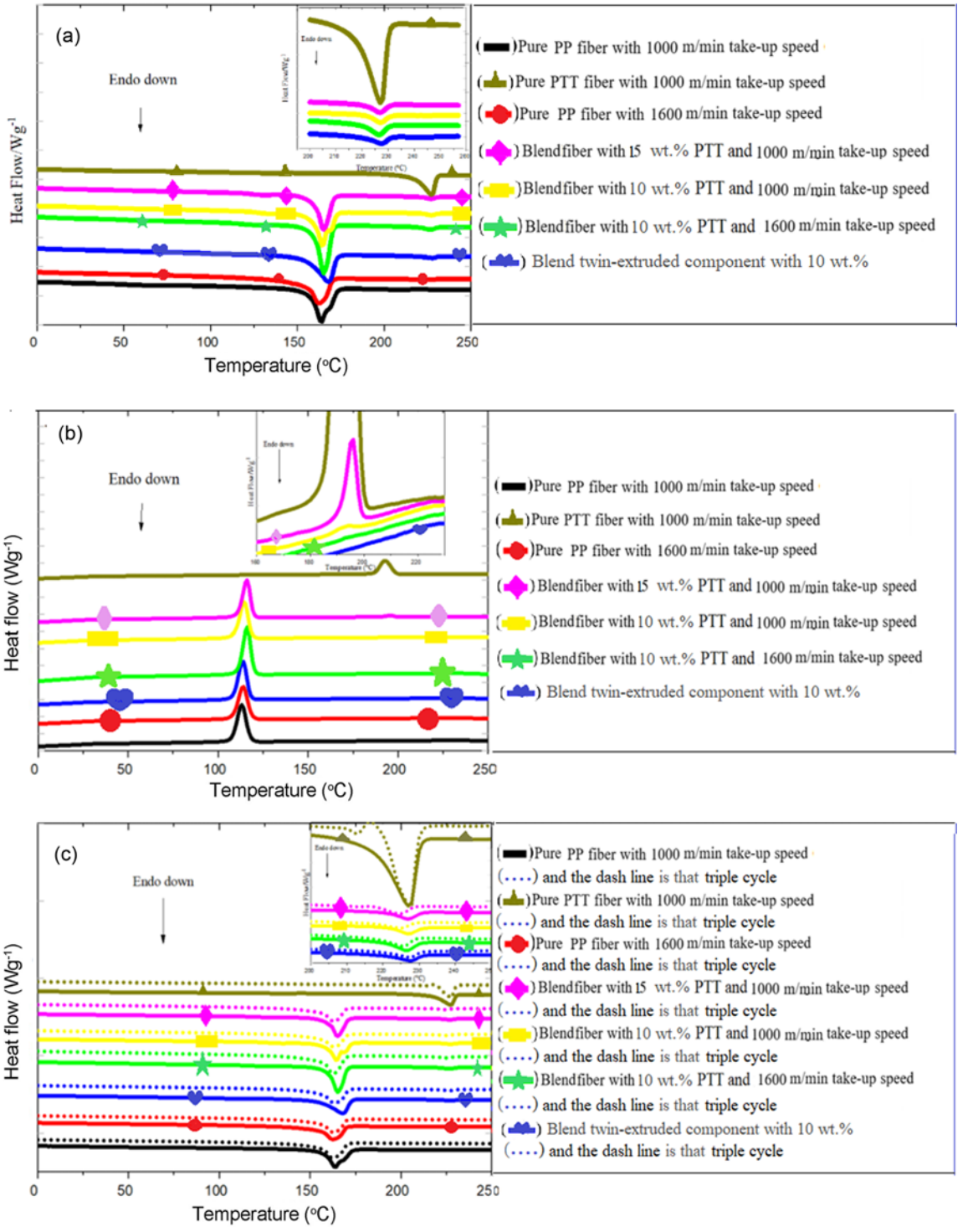

Figure 6. DSC curves of samples.

temperature (T_m), heat of fusion (H_m), heat of crystallinity and degree of crystallinity (X_c) are summarized in Table 2. The pristine PTT FDY fiber exhibited a T_m of 227.3 °C, whereas the PP fiber showed its corresponding Tm is around 164.6 °C at 1000 m/min take up speed which are close to those reported for pristine PP and PTT in the literature [21]. As expected, the results have indicated that the pristine PP and PTT have separated distinct endothermic peak.

Table 2. Summary of the DSC results of pure PP, PTT and the PP/PP-g-MAH/PTT blend samples in first cycle

PP: PP-g-MAH: PTT with different compositions	T_m (°C)		T_c (°C)		$\Delta T=T_m-T_c$ (°C)		ΔH_m (W/g)		Xc (%)	
	PP	PTT	PP	PTT	PP	PTT	PP	PTT	PP	PTT
0:0:100, LOY, 1000 m/min	-	227.3	-	192.6	-	34.7	-	63.9	-	54.8
100:0:0, LOY, 1000 m/min	164.6	-	113.0	-	51.6	-	142.9	-	69.0	-
86:4:10, LOY, 1000 m/min	165.3	225.1	114.6	195.0	50.7	30.1	125.6	4.8	70.5	33.0
81:4:15, LOY, 1000 m/min	164.6	227.0	116.0	196.0	48.6	31	117.6	6.3	74.8	28.9
100:0:0, LOY, 1600 m/min	163.9	-	113.7	-	50.2	-	148.2	-	71.6	-
86:4:10, LOY, 1600 m/min	165.3	227.0	116.0	195.1	49.3	31.9	157.8	8.1	84.7	55.6
86:4:10, M.B, twin-extrude	167.7	228.0	113.6	195.5	54.1	32.5	145.3	6.0	81.6	41.2

Table 3. Summary of the DSC results of pure PP, PTT and the PP/PP-g-MAH/PTT blend samples in third cycle

PP: PP-g-MAH: PTT with different compositions	T_m (°C)		T_c (°C)		$\Delta T=T_m-T_c$ (°C)		ΔH_m (W/g)		Xc (%)	
	PP	PTT	PP	PTT	PP	PTT	PP	PTT	PP	PTT
0:0:100, LOY, 1000 m/min	-	226.7	-	192.6	-	34.1	-	79.8	-	54.9
100:0:0, LOY, 1000 m/min	162.1	-	113.4	-	49.1	-	171.3	-	82.7	-
86:4:10, LOY, 1000 m/min	164.3	225.0	114.6	195.0	49.7	30.0	153.1	5.2	86.0	35.7
81:4:15, LOY, 1000 m/min	162.7	226.0	116.0	196.0	46.7	30.0	165.4	6.4	88.8	29.3
100:0:0, LOY, 1600 m/min	162.5	-	113.7	-	48.8	-	173.0	-	83.0	-
86:4:10, LOY, 1600 m/min	165.0	226.0	116.0	195.1	49.0	30.9	157.8	8.8	88.7	60.5
86:4:10, M.B, twin-extrude	163.1	227.4	113.6	195.5	49.5	31.9	161.8	6.0	90.9	44.7

Furthermore, they show a large difference between solubility parameters and that been dissolved only in solvents with different polarities. However, by adding the PP-g-MA compatibleizer, the compatibility would be enhanced during the reaction between the maleic anhydride and PTT's hydroxyl group is occurred during the melt-processing [32,33]. In the case of PP/PP-g-MA/PTT blend fiber with 86/4/10 percent contain two distinct melting endotherms peaks were observed around 225.1 °C and 165.3 °C, respectively. Furthermore, our data indicated that the T_m and T_c (inset picture illustrated in Figures 6(a) and (b), respectively) became closer by adding the PTT (ΔT=48-49 °C for blend fiber, ΔT=51.6 °C for pristine PP, Table 1). Hence, the crystallization kinetics of PP was increased by the presence of the PTT as a nucleating agent in the PP/PP-g-MA/PTT blend fibers. The same results have been presented by other scientists that indicated the presence of dispersed phase can accelerate the polymer matrix crystallization percentage, especially in nano-size structures [22,25,34-38]. Xue *et al.* [32] indicated that the PTT phase particles, having a T_c of 192.5 °C were already solids at the PP crystallization temperature and could serve as heterogeneous nucleation sites that could benefit the crystallization of PP. Thus, according to Table 2, the crystalline percentage (X_C) of the blend fiber with the compatibleizer using the DSC method was more than that corresponding to the X_C of pristine PP FDY fibers. Also, an increase in the take-up speed in the melt-spinning process increased the X_C, especially in the blend fibers (an approximate 16 %), owning to the rise of draw load [39]. Furthermore, the DSC studies approve that the crystallinity percentage of twin extruded components was more than blend fibers because of high cooling speed in melt-spinning process. Repetition of blend melting converts PTT microfibrils to droplet morphology (as is shown in Figure 6(c) and its inset picture and Table 3). The increase of cooling rate significantly diminishes the percentage of crystallinity in the spinning process compared to DSC method. This evidence leads to higher number of PP crystals in the third cycle rather than those in the first cycle.

Wide-angle X-ray Diffraction

Figure 7(a) shows the wide-angle X-ray scattering (WAXS) patterns of pristine PP and PTT in form of LOY and FDY fiber, respectively. The results are summarized in Table 4. It could be found that the XRD patterns of pristine PP and PP blends display five sharp peaks at 2θ for 14 ° to 28 °. This crystal type corresponds to α monoclinic structure form of isotactic PP that consists of this study results for partially crystalline PP. Structural parameters a, b, c and β=6.65, 20.96, 6.50 A° and 99.38 ° describe crystal instruction [40]. The results showed that XC and ACS values of LOY fiber are higher than those of the FDY fibers. It might be attributed to the differences between the solidification process-temperature and tension through melt-spinning and

hot-drawing process.

There was negligible diffraction in XRD pattern related to LOY and FDY of PTT structure as shown in Figure 7(a) which indicated the absence of detectable crystallinity [41]. This phenomenon is related to the rigid chemical and helical structure of PTT, respectively. It means that the lower cooling rate of molten PTT through the crystallization in comparing with molten PP is very significant for high crystalline regions in the melt -spinning process [42-44].

Table 4. X-ray diffraction spectrum of PP, PTT, PP/PP-g-MAH/ PTT blend samples

PP: PP-g-MAH: PTT with different compositions	ACS at 2θ (Å)	Crystallinity (%)
76:4:20, Blend Master Bach	178.5	78.1
100:0:0, Pure LOY, speed=1000 m/min	96.6	70.6
86:4:10, Blend LOY, speed=1000 m/min	91.6	75.1
76:4:20, Blend LOY, speed=1000 m/min	85.5	76.7
100:0:0, Pure FDY, speed=1000 m/min	87.6	68.1
86:4:10, Blend FDY, speed=1000 m/min	85.0	72.8
76:4:20, Blend FDY, speed=1000 m/min	83.5	74.9
86:4:10, Blend FDY, speed=1600 m/min	180.5	75.1
86:4:10, Blend LOY, speed=1600 m/min	170.9	81.7

The XRD pattern of LOY pristine PP and PP/PP-g-MAH/ PTT blend with percent contain 86/4/10 and 76/4/20 wt %. at take-up speed of 1000 m/min XRD pattern are shown in Figure 7(b) and Table 4. As can be seen, the results of blend fibers and pristine PP showed the same trend. It should be mentioned that the crystalline percentage of PP/PP-g-MA/ PTT blend fiber with increasing of PTT percentage is higher than pristine fibers (~6.3-8.6 %) due to the nucleation of PTT which was confirmed by the results of DSC. However, the crystal size slightly was reduced because of the presence of PDP (~4.6-11.1 %). The same results have been reported previously by some reporter [16,32,36]. Rizivi *et al.* [29] attributed the appearance of the additional peaks in PP due to the effect of second component (*i.e.* PET) acts as a nucleating agent in blend fibers.

It is also noted that an increase in the take-up speed in the melt-spinning process improved the X_C and ACS values, especially in the blend fibers in form of LOY and FDY fiber blend samples as shown in Figure 7(c), due to the rise of draw load which was confirmed by the results of DSC. The same results have been reported previously by Adar and Noether [39] and Paradkar *et al.* [45].

Moreover, ACS values and crystalline percentage of twin-extruded components seem higher than the blend fibers as shown in Figure 7(d) and Table 4, due to higher cooling speed than DSC testes is applied in the melt-spinning.

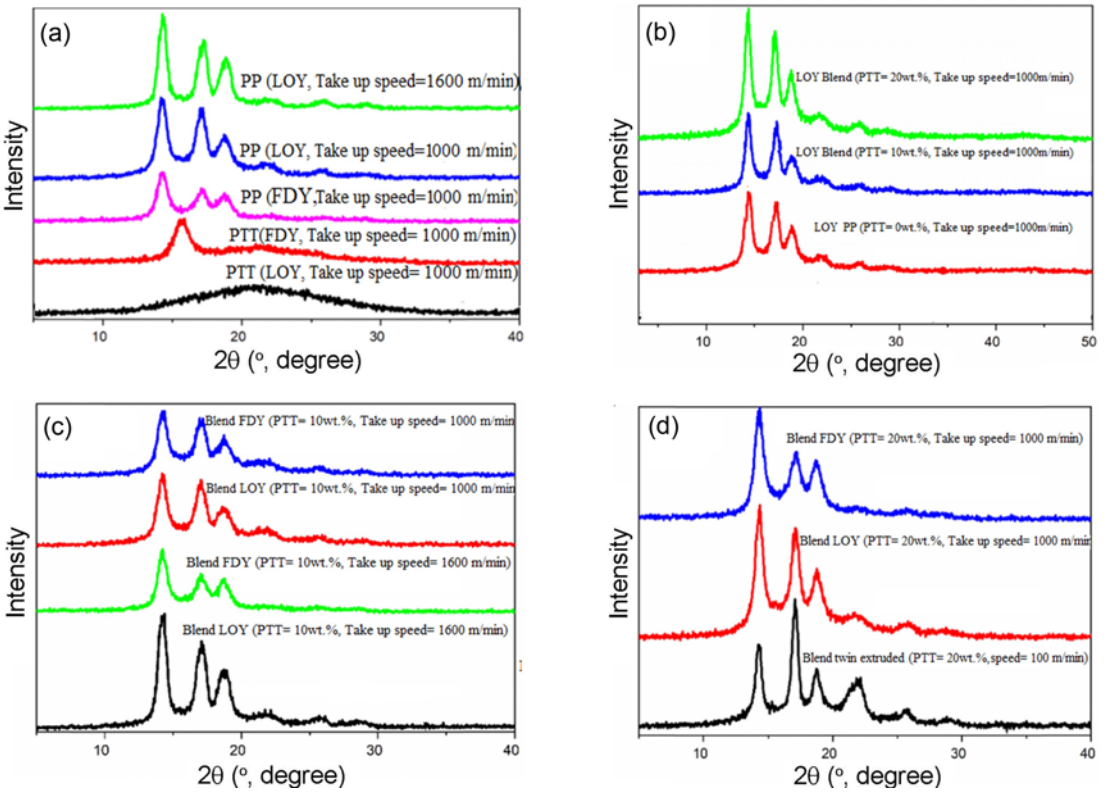

Figure 7. Wide-angle X-ray scattering traces of samples; (a) pristine PP, PTT (b) LOY PP, Blends, (c) LOY and FDY of Blends, and (d) LOY, FDY and Twin extruded of Blends.

Table 5. Effect of blend ratio and take-up speed on the mechanical properties of LOY and FDY samples

PP: PP-g-MAH: PTT with different take-up speed	Tenacity (cN/Tex)		Elongation at break (%)		Modulus (cN/Tex)		Work of rupture (cN/Tex)	
	LOY	FDY	LOY	FDY	LOY	FDY	LOY	FDY
100:0:0, 1000 m/min	10.8 (2.4) *	33.3 (1.6)	432.1 (3.7)	37.9 (3.4)	39.2 (2.3)	181.9 (1.6)	36.6 (6.3)	13.3 (8.9)
91:4:5, 1000 m/min	9.9 (5.6)	32.6 (1.9)	428.7 (4.9)	37.8 (3.0)	37.3 (0.8)	177.0 (1.8)	35.7 (5.1)	13.2 (11.1)
86:4:10, 1000 m/min	9.9 (6.8)	32.5 (2.5)	416.7 (4.2)	38.5 (10.4)	36.2 (4.3)	174.5 (1.1)	33.4 (6.9)	13.1 (9.1)
81:4:15, 1000 m/min	9.9 (4.2)	32.1 (1.6)	408.8 (4.8)	35.8 (4.9)	36.7 (5.5)	172.6 (1.7)	33.7 (1.5)	11.1 (11.2)
76:4:20, 1000 m/min	10.1 (3.0)	32.5 (1.9)	408.9 (7.6)	35.4 (4.6)	36.4 (2.2)	174.9 (9.6)	33.8 (4.7)	10.4 (9.6)
0:0:100, 1000 m/min	7.2 (7.4)	28.0 (2.0)	327.2 (4.5)	48.2 (3.8)	19.8 (7.2)	103.6 (1.1)	12.6 (8.9)	7.9 (6.3)
100:0:0, 1300 m/min	11.8 (3.3)	36.6 (1.4)	421.5 (2.8)	36.9 (5.6)	42.0 (3.8)	204.4 (1.7)	37.6 (5.2)	13.9 (10.7)
91:4:5, 1300 m/min	11.0 (2.8)	35.7 (1.4)	389.4 (5.0)	32.3 (6.9)	40.8 (1.4)	204.4 (1.1)	35.8 (4.2)	8.8 (12.7)
86:4:10, 1300 m/min	10.9 (4.7)	35.8 (3.5)	388.7 (6.0)	33.0 (4.5)	40.6 (1.7)	204.1 (1.1)	34.7 (7.5)	9.6 (13.7)
81:4:15, 1300 m/min	10.6 (6.3)	36.2 (2.9)	377.1 (6.1)	31.1 (5.1)	40.7 (3.4)	201.9 (2.0)	35.4 (9.0)	8.9 (12.3)
76:4:20, 1300 m/min	10.6 (4.2)	34.1 (6.8)	373.6 (6.8)	32.3 (9.4)	39.1 (2.3)	188.5 (9.3)	33.3 (3.3)	9.1 (1.6)
0:0:100, 1300 m/min	8.8 (3.9)	30.1 (6.8)	319.9 (10.5)	44.3 (3.2)	24.1 (3.8)	124.2 (4.9)	13.3 (12.3)	8.3 (11.1)
100:0:0, 1600 m/min	12.0 (4.4)	39.2 (2.4)	395.0 (5.7)	33.8 (9.9)	44.7 (2.1)	224.3 (1.2)	39.3 (3.1)	9.2 (12.5)
91:4:5, 1600 m/min	11.6 (5.4)	38.4 (2.6)	354.3 (9.0)	34.9 (4.9)	44.5 (3.9)	219.9 (3.5)	34.8 (4.0)	10.7 (12.3)
86:4:10, 1600 m/min	11.4 (2.9)	39.5 (0.7)	359.3 (5.1)	33.7 (3.5)	44.5 (4.1)	220.3 (1.3)	32.5 (4.9)	9.7 (13.4)
0:0:100, 1600 m/min	8.9 (1.7)	29.2 (7.9)	315.1 (6.1)	42.1 (3.9)	24.3 (1.3)	129.9 (2.1)	13.4 (4.2)	8.7 (8.8)

*Values inside brackets indicate percent coefficient of variation.

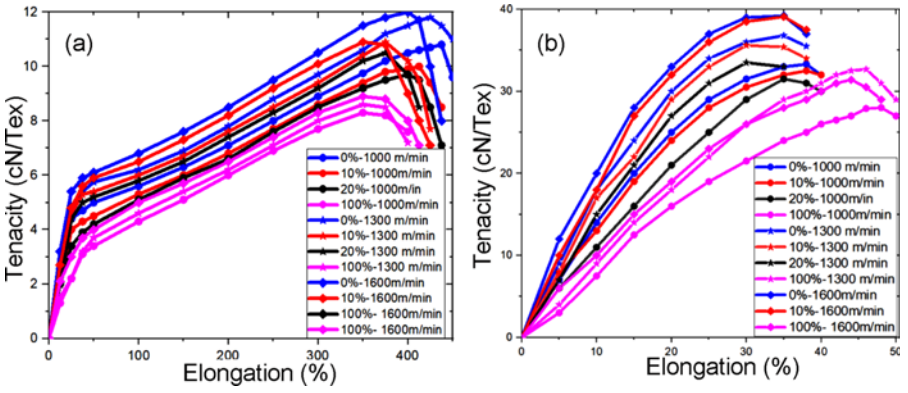

Figure 8. Tenacity-elongation curves of the PTT fibers LOY (a) and FDY (b) prepared at different take-up velocities.

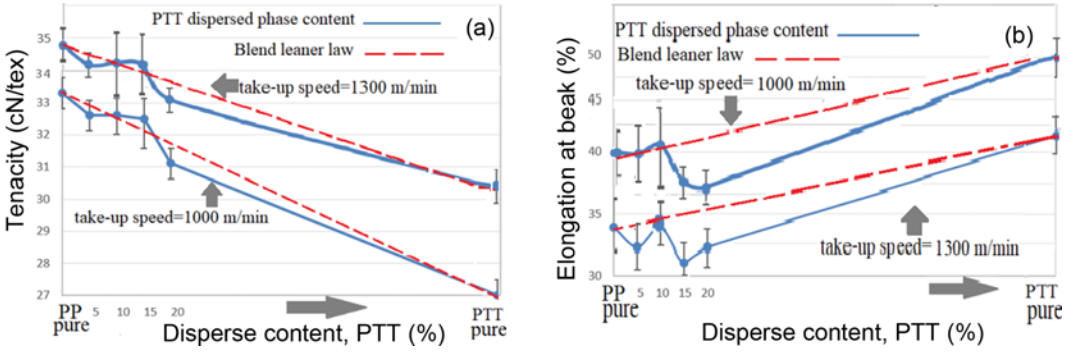

Figure 9. Tenacity (a) and elongation at beak (b) deviation of PP/PP-g-MAH/PTT from blends linear law with increasing of the PTT content.

Mechanical Properties Evaluations

Mechanical properties of as-spun (LOY) and post hot-drawn (FDY) fibers are compared in Table 5 and Figure 8(a) and 8(b). Measured values are for both pristine and blend fibers produced at three different take-up speeds (1000, 1300 and 1600 m/min). The most regular elongation at break is for FDY fibers series belonging to the pristine PTT special zigzag structure [11-13]. The as-spun pristine PTT fiber showed the lowest amount of mechanical properties and the as-spun pristine PP presented the highest. The same results have been reported by another scientist [19,25]. Based on the mixture law [23], as it is expected, increasing the PDP to the PP matrix phase resulted in decreasing the mechanical properties of blend samples in comparison with the pristine PP samples.

Within LOY and FDY series, the mechanical properties behavior of PP/PP-g-MA/PTT blends were less than the pristine PP but the behavior of the blend sample with the ratio of 91/4/5 was similar to that of PP. Lin *et al.* [16] claimed that the addition of second component (*e.g.* PTT) could inhibit the formation of β-crystal structures, however good mechanical properties were expected to be in the isotactic PP. The variation of mechanical properties was not negligible for 20 % of PTT. These trends were quite obvious regarding the studies of Kurian [12] and Patel [15] analyses which indicate that the mechanical properties of PTT is significantly lower than that of other commercial polymers, especially PP. Therefore, these results could be predicted according to the mixture law [44]. The fluency of melting-process is also important for the filament yarns to gain suitable spinability and acceptable mechanical properties [23]. More than 20 % of PTT were prepared by some researchers [17,19,32]. This fact could be attributed to the Maddock fluted mixing zone on the extruder screw, and their production speed is far from industrial melt-spinning devices which have lower shear stress. The main aim of this work is to optimize the components ratio in blends and to achieve favorable-industrial scale and tailored properties of the blends [47-49].

The best tenacity in the FDY blend fibers at 1300 and 1000 m/min take-up speed were indicated for the 15 and 10 % PTT content, respectively, and the same results for the elongation at break were obtained at 1000 m/min take-up speed as shown in Figures 9(a) and 9(b). The deterioration of the mechanical properties for the 20 % PTT blend fiber can be related to the significant irregularity of the fibril's diameters, demonstrated by the morphological evaluations of the blends with the higher coefficient of variation with 20 % PTT [12].

Optimization of Fibers Mechanical Properties

Pre-experiments guide that PTT, PP-g-MA compatibleizer and take-up speed are most efficient parameters in melt-spinning process. These principles make desirable industrial scale features such as fine constant spin-ability and strong mechanical properties. Therefore, a Box-Behnken design (BBD) as a second-order multivariate technique [20] based on three-level factors was designed in order to model the process (with the three mentioned factors). The highest and the lowest levels of those parameters were determined by pre-experiments. According to BBD with three factors, it was necessary to have 17 tests conducted. A regression mathematical model was developed for predicting the mechanical properties of fibers. Also, the analysis of variance (ANOVA), presents high coefficient correlation and no significant lack of fit which demonstrate that the variation in the mechanical properties could be explained reasonably by the quadratic equations. The modified regression equation and R square parameter were obtained with p value < 0.05 as equations (3)-(6):

$$T = -6.58 + 0.24X_1 + 0.01\,X_3 - 0.39(X_2)_2 - 3.79E-006(X_3)^2,\ R^2=0.93 \quad (3)$$

$$E = 404.00 - 2.02X_1 - 0.11X_3 + 2.85E-003X_1X_3 - 8.91X_2X_3 - 0.15(X_1)^2 - 7.84(X_2)^2,\ R^2=0.99 \quad (4)$$

$$M = 12.42 + 6.49E-003X_3 + 1.67E-003X_2X_3 + 0.03(X_1)^2 - 1.51(X_2)^2,\ R^2=0.99 \quad (5)$$

Table 6. Results of experimental design

Run	X_1 (%)	X_2 (%)	X_3 (m/min)	Tenacity (cN/Tex)	Elongation at break (%)	Modulus (cN/Tex)	Work of rupture (cN/Tex)
1	10	4	1300	10.9	388.7	40.6	34.7
2	15	5	1300	10.0	371.8	39.4	33.2
3	10	4	1300	11.5	389.9	40.1	35.1
4	10	3	1000	9.5	412.7	35.8	32.1
5	10	4	1600	11.4	359.3	44.5	32.5
6	15	4	1000	9.9	408.8	36.7	33.7
7	5	5	1300	10.9	382.1	39.3	35.2
8	15	3	1300	10.2	374.2	39.9	33.9
9	10	3	1600	11.1	351.8	42.1	30.1
10	5	4	1000	9.9	428.7	37.3	35.7
11	10	4	1300	10.8	389.6	40.1	34.1
12	10	5	1600	11.0	344.2	42.5	30.2
13	10	4	1300	10.7	389.2	39.9	34.1
14	10	5	1000	9.4	415.8	34.2	32.5
15	5	4	1600	11.6	354.3	44.5	34.8
16	15	4	1300	10.6	377.1	40.7	35.4
17	5	3	1300	10.9	385.4	39.6	35.4

Table 7. Optimized conditions, predict and experimental values, and absolute percentage errors optimum

Values of	X_1 (%)	X_2 (%)	X_3 (m/min)	Tenacity (cN/Tex)	Elongation at break (%)	Modulus (cN/Tex)	Work of rupture (cN/Tex)
Experimental	9.3	3.8	1092.6	10.6 (7.4) *	420.3 (6.8)	38.1 (1.5)	36.1 (8.2)
Predicted	9.3	3.8	1092.6	10.3 (3.3)	412.6 (3.7)	37.7 (0.8)	34.2 (5.1)
Absolute error (%)				2.8	1.8	4.9	5.3

*Values inside brackets indicate percent coefficient of variation. The model present for the significant terms, p value < 0.05 and vice versa.

$$W = -15.56 + 0.05X_3 - 1.92X_2X_3 + 0.05(X_1)^2 - 1.38(X_2)^2, \quad R^2 = 0.97 \tag{6}$$

where T, E, M and W are the average tenacity (cN/Tex), Elongation at break (%), Modulus (cN/Tex) and Work of rupture (cN/Tex), respectively. X_1 is the concentration of PTT (%), X_2 is used for concentration of PP-g-MA and X_3 shows the take-up speed in the melt-spinning process (X3, m/min). The experimental results of LOY fibers were obtained from the model presented in Table 6.

According to the modified model, the average mechanical properties of LOY blend fibers were optimized. The optimal values in terms of concentration of PTT polymer, PP-g-MA compatibleizer and take-up speed parameters were predicted. The optimal mechanical properties using rule of mixture was dependent on this value: 9.3 % PTT, 3.8 % PP-g-MA compatibleizer and 1092 m/min take-up speed (as presented in Table 7) which confirms the results of the predicted rule of mixtures. According to the predicted model, there were 10.3 cN/Tex for tenacity, 412.6 % for elongation at break, 37.7 cN/Tex for modulus and 34.2 cN/Tex for work of rupture It means that coefficient percentage of variation at optimized conditions were evaluated with the predicted values. As presented in Table 6, the experimental average mechanical properties were compared with the coefficient percentage of variation for optimum values (10.6, 420.3 %, 38.1 cN/Tex, 36.1 cN/Tex). Similar data of both methods confirms the accuracy of the model. As shown in Figure 10(a-l), it could be observed that an increase of the concentration of the PTT (X_1) and PP-g-MA compatibleizer (X_2) would result in a decrease of tenacity of LOY fiber blend while the increase of take-up speed (X_3) has the opposite effect. The effects of PTT and PP-g-MA concentration on the blend tenacity matches the result of various reports [8,16,19]. Our results suggest that take-up speed plays a key role in the spin-ability and mechanical properties behavior of PP/PP-g-MA/PTT blend fibers. As can be seen, range of 3-5 % of PP-g-MA compatibleizer has a negligible role in

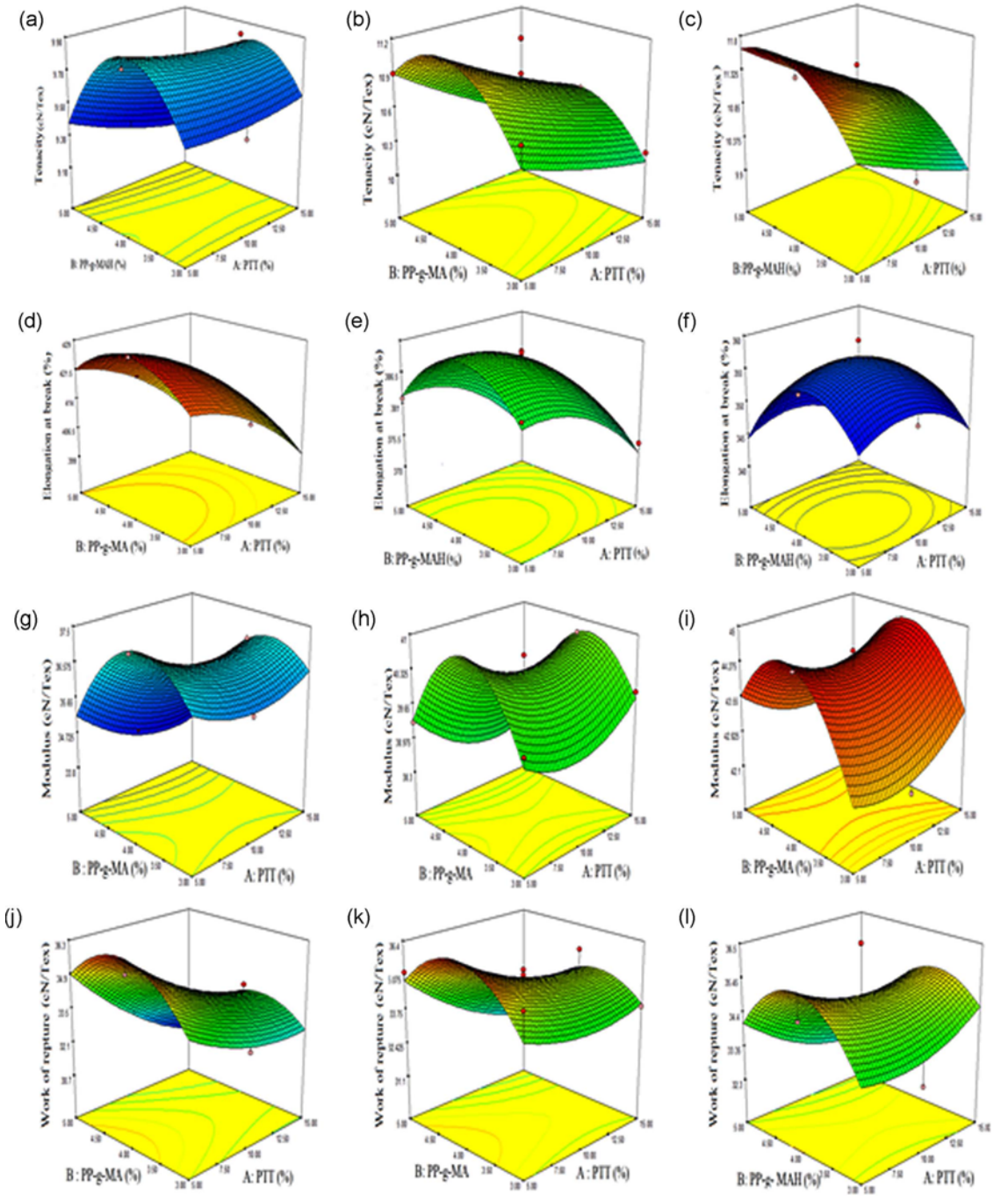

Figure 10. 3D surface for tenacity (a, b, c), Elongation at break (d, e, f), Modulus (g, h, i), Work of rapture (j, k, l).

mechanical properties of LOY fiber blends compared to the concentration of PTT and take-up speed in melt spinning process. Teli and Desai [8] reported that the maximum tenacity was observed for 3 % PP-g-MA compatibleizer and further addition *i.e.* 5 % PP-g-MA compatibleizer led to decrease in tenacity due to this fact that molecular weight of PP matrix would be reduced.

Conclusion

The rheological behavior results helped to demonstrate and confirm the fibrillation of PTT domains in PP matrix. The complex viscosity and storage modulus of the PP/PP-g-MA/PTT blend fibers increased by increasing the amount of PTT via a network structure in low frequencies. The

development of the fibrillar structures were gained at different steps of melt spinning process. The distributions of PTT fibrils were evaluated using SEM indicated that the lowest average diameter of nano-fibrils was about 64 nm which is appropriated to FDY blend fiber samples consisting of 10 wt% of PTT. Moreover, a positive deviation is obtained from mixture law. The best tenacity and elongation at break degree is reported for FDY samples with 10 % of PTT amount. The DSC and XRD results considerably influenced the crystallinity of PP by presence of PTT. The optimized blend fiber in this research could be considered as a promising nomination for a broad range of practical use from apparel to carpet.

References

1. M. Ataeefard, M. Mohseni, and S. Moradian, *J. Text. Inst.*, **107**, 182 (2016).
2. D. W. Sauter, M. Taoufik, and C. Boisson, *Polymers*, **9**, 185 (2017).
3. M. A. Tavanaie, A. M. Shoushtari, and F. Goharpey, *J. Clean. Product.*, **18**, 1866 (2010).
4. M. L. Xue, Y. L. Yu, H. H. Chuah, J. M. Rhee, N. H. Kim, and J. H. Lee, *Eur. Poly. J.*, **43**, 3826 (2007).
5. J. Rosch and R. Mulhaupt, *Makromol. Chem-Rapid. Com.*, **14**, 503 (1993).
6. Y. Tao and K. Mai, *Eur. Poly. J.*, **43**, 3538 (2007).
7. K. Dobrovszky, *Periodica Polytechnica. Mech. Eng.*, **55**, 73 (2011).
8. M. D. Teli and P. V. Desai, *Int. Res. J. Eng. Tech.*, **2**, 396 (2015).
9. F. P. L. Mantia, M. Ceraulo, G. Giacchi, M. C. Mistretta, and L. Botta, *Polymers*, **9**, 47 (2017).
10. S. Aparna, D. Purnima, and R. B. Adusumalli, *Poly.-Plast. Tech. Eng.*, **56**, 617 (2017).
11. M. R. H. Zargar and A. M. Shoushtari, *J. Macromol. Sci., Part B*, **58**, 141 (2019).
12. J. Dong, A. Huang, J. Sun, L. Wei, S. Luo, and S. Qin, *Poly. Com.*, **40**, E629 (2019).
13. H. Liu, Y. Xu, Z. Zheng, and D. Liu, *Biotech. J.*, **5**, 1137 (2010).
14. H. Przystalowska, D. Lipiński, and R. Slomski, *Act. Biochim. Polonica*, **62**, 23 (2015).
15. H. A. Khonakdar, M. A. Ehsani, A. Asadinezhad, S. H. Jafari, and U. Wagenknecht, *J. Macromol. Sci., Part B: Phys.*, **52**, 897 (2013).
16. Z. Lin, B. Xu, Z. Guan, and C. Chen, *J. Ind. Eng. Chem.*, **19**, 926 (2013).
17. J. Liu and X. Zhu, *Polym. Eng. Sci.*, **59**, E317 (2019).
18. A. Ujhelyiova, E. Bolhova, J. Oravkinova, R. Tiňo, and A. Marcinčin, *Dyes Pigm.*, **72**, 212 (2007).
19. S.-W. Lin and Y.-Y. Cheng, *Poly.-Plastics Tech. Eng.*, **48**, 827 (2009).
20. B. Rezaei, M. Askari, A. M. Shoushtari, and R. A. M. Malek, *J. Thermal Anal. Calorimetry*, **118**, 1619 (2014).
21. S. H. Jafari, A. Kalati, H. A. Khonakdar, A. Asadinezhad, U. Wagenknecht, and D. Jehnichen, *Exp. Polym. Lett.*, **6**, 148 (2012).
22. A. Esfandiari, H. Nazockdast, A. S. Rashidi, and M. E. Yazdanshenas, *J. Appl. Sci.*, **8**, 545 (2008).
23. M. A. Tavanaie, A. M. Shoushtari, F. Goharpey, and M. R. Mojtahedi, *Fiber. Polym.*, **14**, 396 (2013).
24. M. Munaro and L. Akcelrud, *J. Polym. Res.*, **15**, 83 (2008).
25. M. Xue, Y. Yu, H. H. Chuah, and G. Qiu, *J. Macromol. Sci., Part B: Phys.*, **46**, 387 (2007).
26. A. Bigdeli, H. Nazockdast, A. Rashidi, and M. E. Yazdanshenas, *J. Polym. Res.*, **19**, 289 (2012).
27. M. A. Tavanaie, A. M. Shoushtari, and F. Goharpey, *J. Macromol. Sci., Part B: Phys.,* **49**, 163 (2010).
28. A. Safaei, M. Masoomi, and S. M. R. Razavi, *Bull. Mat. Sci.*, **40**, 971 (2017).
29. A. Rizvi, Z. K. M. Andalib, and C. B. Park, *Polymer*, **110**, 139 (2017).
30. M. V. Tsebrenko, N. M. Rezanova, and G. V. Vinogradov, *Polym. Eng. Sci.*, **20**, 1023 (1980).
31. M. Afshari, R. Kotek, M. H. Kish, H. N. Dast, and B. S. Gupta, *Polymer*, **43**, 1331 (2002).
32. M. L. Xue, Y. L. Yu, and H. H. Chuah, *J. Macromol. Sci., Part B: Phys.*, **46B**, 603 (2007).
33. Y. Wang and M. Run, *J. Poly. Res.*, **16**, 725 (2009).
34. S. Acierno, R. Barretta, R. Luciano, F. Marotti de Sciarra, and P. Russo, *Compos. Struct.,* **174**, 12 (2017).
35. M. Krištofič and A. Ujhelyiová, *Fibers Text. East. Eur.*, **93**, 30 (2012).
36. X. Si, L. Guo, Y. Wang, and K. Lau, *Compos. Sci. Tech.*, **68**, 2943 (2008).
37. A. Szymczyk, Z. Roslaniec, M. Zenker, M. C. García-Gutiérrez, J. J. Hernández, D. R. Rueda, A. Nogales, and T. A. Ezquerra, *Exp. Polym. Lett.*, **5**, 977 (2011).
38. X.-F. Xia, J.-H. Zhang, J.-M. Fan, Q.-L. Jiang, and S.-A. Xu, *Int. J. Poly. Anal. Character.*, **21**, 697 (2016).
39. F. Adar and H. Noether, *Polymer*, **26**, 1935 (1985).
40. A. Bigdeli, H. Nazockdast, A. Rashidi, and M. E. Yazdanshenas, *J. Macromol. Sci., Part B: Phys.*, **55**, 732 (2016).
41. G. Wu, H. Li, Y. Wu, and J. A. Cuculo, *Polymer*, **43**, 4915 (2002).
42. J. Hu, J. Lu, and Y. Zhu, *Poly. Rev.*, **48**, 275 (2008).
43. J. Wu, J. M. Schultz, J. M. Samon, A. B. Pangelinan, and H. H. Chuah, *Polymer*, **42**, 7141 (2001).
44. G. Mingliang, J. Demin, and X. Weibing, *Poly.-Plast. Tech. Eng.*, **46**, 985 (2007).
45. M. R. P. Paradkar, S. S. Sakhalkar, and X. H. Center, *J. Appl. Polym. Sci.*, **88**, 545 (2003).
46. J. V. Kurian, *J. Polym. Environ.*, **13**, 159 (2005).
47. M. R. Habibolah Zargar and A. M. Shoushtari, *J. Macromol. Sci., Part B: Phys.*, **58**, 723 (2019).
48. M. R. Habibolah Zargar and A. M. Shoushtari, *J. Macromol. Sci., Part B: Phys.*, **58**, 141 (2019).
49. R. Hajiraissi, *Poly. Bull.*, **77**, 2423 (2019).